



Intratumoral Injection of Large Surface Area Microparticle Taxanes in Carcinomas Increases Immune Effector Cell Concentrations, Checkpoint Expression, and Synergy with Checkpoint Inhibitors: A Review of Preclinical and Clinical Studies

Gere S. diZerega · Holly A. Maulhardt · Shelagh J. Verco ·
Alyson M. Marin · Michael J. Baltezor · Samantha A. Mauro ·
Marc A. Iacobucci

Received: November 3, 2023 / Accepted: January 4, 2024
© The Author(s) 2024

ABSTRACT

This review summarizes development of large surface area microparticle paclitaxel (LSAM-PTX) and docetaxel (LSAM-DTX) for local treatment of primary carcinomas with emphasis on immunomodulation. Intratumoral (IT) delivery of LSAM-PTX and LSAM-DTX provides continuous, therapeutic drug levels for several weeks. Preclinical studies and clinical trials reported a reduction in tumor volume (TV) and immunomodulation in primary tumor and peripheral blood with increases in innate and adaptive immune cells and decreases in suppressor cells. Increased levels of checkpoint expression of immune cells occurred in clinical trials of high-risk non-muscle-invasive bladder

cancer (LSAM-DTX) and unresectable localized pancreatic cancer (LSAM-PTX). TV reduction and increases in immune effector cells occurred following IT LSAM-DTX and IT LSAM-PTX together with anti-mCTLA-4 and anti-mPD-1, respectively. Synergistic benefits from combinatorial therapy in a 4T1-Luc breast cancer model included reduction of metastasis with IT LSAM-DTX + anti-mCTLA-4. IT LSAM-PTX and LSAM-DTX are tumoricidal, immune enhancing, and may improve solid tumor response to immune checkpoint inhibitors without additional systemic toxicity.

Keywords: Paclitaxel; Docetaxel; Intratumoral injection; Intraprostatic injection; Intramural injection; Intravesical instillation; Immunomodulation; Pancreatic cancer; Prostate cancer; Urinary bladder cancer; LSAM-DTX; LSAM-PTX

G. S. diZerega (✉) · H. A. Maulhardt ·
S. J. Verco · A. M. Marin · S. A. Mauro
US Biotest, Inc., 231 Bonetti Drive, Suite 240, San
Luis Obispo, CA 93401, USA
e-mail: gere.dizerega@usbiotest.com

G. S. diZerega · M. A. Iacobucci
NanOlogy, LLC., 3909 Hulen Street, Fort Worth,
TX 76107, USA

M. J. Baltezor
CritiTech, Inc., 1849 E 1450 Road, Lawrence, KS
66044, USA

Key Summary Points

Local administration of chemotherapy has the potential to reduce side effects typical of IV chemotherapy and provides higher amounts of drug in the tumor for longer durations which increases tumor kill.

This paper reviews recent results of human trials of localized prostate cancer, bladder cancer, and pancreatic cancer treated with locally administered large surface area microparticle docetaxel (LSAM-DTX) or paclitaxel (LSAM-PTX) and animal studies which show that locally administered LSAM-PTX or LSAM-DTX + immunotherapy improved tumor response.

Based on recent evidence that combination therapy will provide better results for more patients, this review provides a call for action to evaluate IT LSAM-PTX or LSAM-DTX followed by IV immunotherapy in patients with solid tumors.

INTRODUCTION

Immunotherapy is an effective treatment option for many carcinomas targeting immune checkpoints within the tumor microenvironment (TME) to enhance tumor cell sensitivity to destruction by the innate and adaptive immune systems [1]. These checkpoints include programmed cell death protein 1 (PD-1), programmed death-ligand 1 (PD-L1), or cytotoxic T-lymphocyte-associated protein 4 (CTLA-4). One of the limitations of immunotherapy is the heterogeneity in treatment responses within and between tumor types [2]. Phenotypic differences within the TME have been classified into three general categories: infiltrated-excluded, infiltrated-inflamed, and tertiary lymphoid structure (TLS) [3]. The infiltrated-excluded category is characterized by the presence of cytotoxic lymphocytes and tumor-associated macrophages in the periphery of the

tumor but not within the tumor. These tumors, of which pancreatic ductal adenocarcinoma is an example, are often immunologically “cold” and lack an effective immune response. The infiltrated-inflamed category is characterized by the invasion of cytotoxic lymphocytes and the expression of PD-1 and PD-L1, interferon- γ (IFN γ), and granzyme B. These tumors are immunologically “hot” and can be found among tumor types with a deficiency in DNA mismatch repair [3]. The TLS category, of which some gastrointestinal carcinomas are examples, is characterized by the presence of T cells, Treg cells, B cells, and dendritic cells (DC) in lymphoid aggregates along the tumor stroma or invasive margin [3–6]. Clinical strategies to improve tumor responsiveness to immunotherapy in all subtypes include combinatorial therapy with other systemic agents to increase cytotoxic T cell infiltration and expression of PD-1, PD-L1, and/or CTLA-4 prior to immunotherapy.

Direct intratumoral (IT) treatment of solid tumors with chemotherapy has the potential to overcome many limitations of conventional intravenous (IV) administration including severe toxicities resulting from systemic distribution [7, 8]. Locally intensive therapies for solid tumors would likely improve treatment efficacy by inducing continuous exposure of tumor cells to therapeutic drug levels over multiple tumor cell-divisions [9, 10]). Various systems for intratumoral treatment of solid tumors are being developed for cancer treatment [11, 12]. However, success is often limited by insufficient IT drug delivery and distribution, limited retention of therapeutic chemotherapy levels within the TME, and emergence of drug resistance by tumor cells [13].

To address these limitations, large surface area microparticle paclitaxel (LSAM-PTX) and docetaxel (LSAM-DTX) were developed (Critech, Inc., Lawrence, KS) to allow for suspension of lipophilic drug particles in a saline-based diluent [14]. These particles have a large surface area which facilitates therapeutic drug release and are of sufficient size for tumor retention. Aqueous suspensions of LSAM-PTX and LSAM-DTX allow for local administration via inhalation, intraperitoneal (IP), intravesical,

intracystic, and IT administration. IT LSAM-PTX and LSAM-DTX result in drug retained in the tumor for several weeks compared to the short exposure time of similar amounts administered IV. Prolonged release of drug provides for continuous release of taxane exposing tumor cells to high, therapeutic levels of drug during multiple mitotic cycles [15, 16].

This review describes the response of various carcinomas to locally administered LSAM-PTX or LSAM-DTX in preclinical studies and clinical trials (Table 1). All institutional and national guidelines for the care and use of laboratory animals were followed. Investigational review boards for all participating clinical sites provided approval for protocol and informed consents for subjects in accordance with the Code of Federal Regulations and local requirements. All procedures followed were in accordance with the ethical standards of the responsible committee on human experimentation (institutional and national) and with the Helsinki Declaration of 1975, as revised in 2000 (5). Informed consent was obtained from all patients for being included in the study. Although all studies show a reduction in tumor volume, as expected for taxanes, the focus here will be on LSAM-PTX- and LSAM-DTX-induced immunomodulation observed in preclinical and clinical trials. Results suggest that IT injection of LSAM-PTX or LSAM-DTX into carcinomas provides clinical benefit with negligible local or systemic toxicity and may enhance responsiveness to immunotherapy. Taken together, the results summarized here support the hypothesis that IT LSAM-PTX and IT LSAM-DTX may provide an important addition to immunotherapies in the treatment of primary carcinomas.

MANUFACTURING PROCESS FOR LSAM TAXANES

Production of taxane microparticles, including LSAM-DTX and LSAM-PTX, by a precipitation with compressed antisolvent (PCA) technique, was previously described [14, 17]. In general, this technology produces particles with a significantly greater specific surface area (SSA) and greater surface/weight ratio than starting drug

substance along with a reduction in bulk density, allowing for homogeneous suspension of the particles for local administration [15, 16]. SSA is a measure of the particle surface area-to-mass ratio and is directly proportional to the rate of drug release from the particles. LSAM-PTX and LSAM-DTX are produced following dissolution of drug substance in a suitable organic solvent and injection into the antisolvent, supercritical fluid carbon dioxide, plus sonication to form uniform droplets (Fig. 1). The solvent is instantaneously stripped from solution with sonic energy resulting in precipitation of LSAM-PTX and LSAM-DTX with a volume-based particle size ranging from 3.5 and 7.5 μm [15]. The sponge-like matrix inside the particles is largely responsible for the increase in surface area. These particles are large enough to avoid being removed by blood flow or phagocytized by macrophages and are retained in tumors following IT injection, creating a depot for sustained drug release [18]. After gamma sterilization, LSAM-PTX and LSAM-DTX are stored as a powder at room temperature and suspended at the time of use in a saline-based diluent for tumor injection. As an example, the LSAM-DTX particles shown in Fig. 2 have a mean particle size of 3.89 μm and SSA of 25.83 m^2/g .

LSAM-DTX: PRECLINICAL GENITOURINARY-ONCOLOGIC XENOGRAFTS

Intratumoral residence time, systemic toxicity, and immune effects of locally administered LSAM-DTX were evaluated in genitourinary-oncologic xenografts in rats and mice. The effects were evaluated in clear cell renal carcinoma (786-O: rats), transitional cell bladder carcinoma (UM-UC-3: mice), and prostate carcinoma (PC-3: mice) xenografts. All groups were administered IT LSAM-DTX, IV docetaxel, and IT vehicle every 7 days with one, two, or three doses administered then followed for tumor growth and clinical observations [19]. In a syngeneic renal cell adenocarcinoma model (Renca-CRL-2947: mice), subcutaneous tumors were treated with 3 weekly cycles of IT vehicle

Table 1 Clinical trials of large surface area microparticle (LSAM) taxanes

Study ID	NCT number	Number of patients	Route of administration	Study title	Study status ^a
LSAM docetaxel (LSAM-DTX)					
NANODOCE-2017-02	NCT03636256	19 (NMIBC), 17 (MIBC)	Direct injection to the bladder wall and intravesical instillation	Phase 1/2 trial evaluating the safety and tolerability of NanoDoce® injection and intravesical instillation in subjects with urothelial carcinoma [30]	Completed
LSAM paclitaxel (LSAM-PTX)					
HSC#1114	NCT00666991	21	Intraperitoneal	Pharmacokinetic, safety and efficacy study of nanoparticle paclitaxel in patients with peritoneal cancers [98]	Completed
NANOPAC-2016-01	NCT03029585	10	Intraperitoneal	Phase II study of four dose levels of intraperitoneal NanoPac Plus IV carboplatin and paclitaxel in patients with epithelial ovarian cancer undergoing cytoreductive surgery [99]	Completed
NANOPAC-2016-02	NCT03077659	16	Intraprostatic injection	Phase IIa dose escalation trial of NanoPac focal therapy for prostate cancer in subjects undergoing radical prostatectomy [16]	Completed
NANOPAC-2017-01	NCT03188991	19	Intracystic injection	A trial evaluating escalating doses and the safety of intracystic injection of NanoPac in subjects with mucinous cystic pancreatic neoplasms [100]	Completed
NANOPAC-2016-05	NCT03077685	54	Intratumoral injection	Phase IIa trial evaluating the safety of intratumoral injection of NanoPac in subjects with locally advanced pancreatic adenocarcinoma [33]	Completed
NANOPAC-2019-01	NCT04221828	1	Intratumoral injection	Phase 2 trial of NanoPac focal therapy for prostate cancer in subjects undergoing radical prostatectomy	Terminated

Table 1 continued

Study ID	NCT number	Number of patients	Route of administration	Study title	Study status ^a
NANOPAC-2020-01	NCT04314895	18	Intratumoral injection	Phase 2 trial evaluating the safety and tolerability of intratumoral injections of NanoPac® with standard of care therapy in subjects with lung cancer	Completed

^aStudy status current as of 24 January 2024

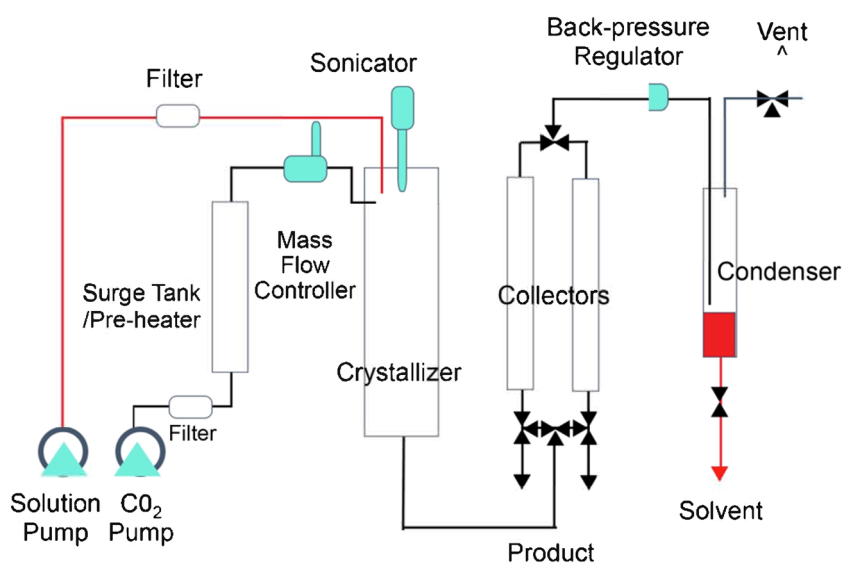


Fig. 1 Schematic of manufacturing process for large surface area particles composed only of taxanes (docetaxel, LSAM-DTX; paclitaxel, LSAM-PTX). Supercritical carbon dioxide (scCO₂) above the critical point (> 72.8 bar, > 31 °C) is utilized in the manufacturing process. scCO₂ is miscible with organic solvents but acts as an antisolvent

for docetaxel which is relatively hydrophobic. Mixing docetaxel in organic solvent with scCO₂ causes LSAM-DTX to precipitate into small particles. These small particles are captured in a filter and dried. Adapted with permission from [15]

or IT LSAM-DTX or 2 weekly cycles of IV docetaxel [18].

Prolonged Taxane Residence in Tumors

IT LSAM-DTX eliminated most tumors and stimulated immune cell infiltration into the tumor site. In contrast, IT vehicle and IV docetaxel elicited limited or no immune cell infiltration. IV docetaxel-treated tumors contained

low (5.10 ng/g) docetaxel levels 50 days post-treatment. In contrast, high levels of docetaxel were present in LSAM-DTX treated tumors 50 days post-treatment. After a single administration of IT LSAM-DTX, docetaxel was detectable in the 786-O and UM-UC-3 tumors in concentrations of 659 ng/g to 144 µg/g and 154 ng/g to 2140 ng/g, respectively, resulting in intratumoral docetaxel concentrations in excess of 30 times greater than following IV administration [19].

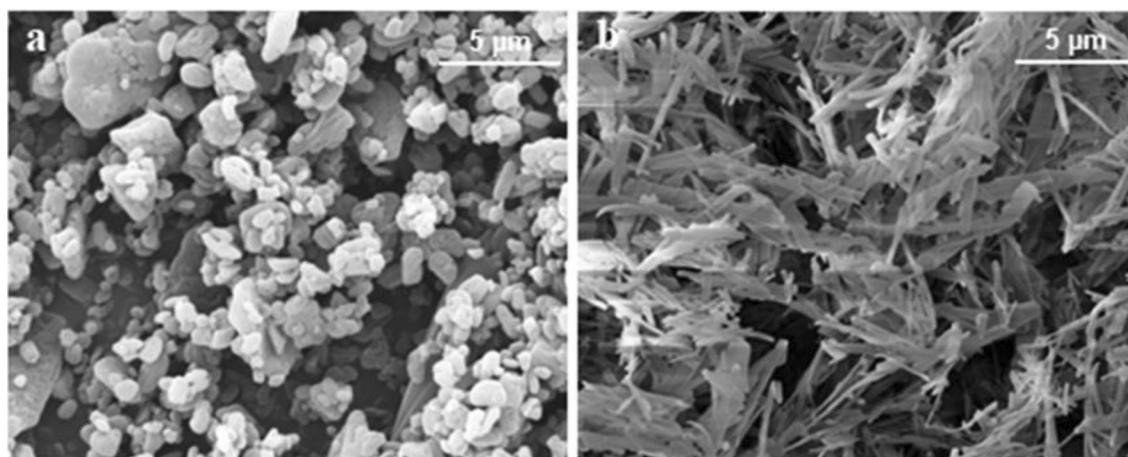


Fig. 2 a Electron micrograph of docetaxel drug substance prior to processing with specific surface area (SSA) 6.98 m²/g and median particle volume (Dv50) 2.85 µm.

b Electron micrograph of large surface area microparticle docetaxel (LSAM-DTX) with SSA 25.83 m²/g and Dv50 3.89 µm. Adapted with permission from [15]

Increased Peripheral Blood Immune Effector Cell Levels

Immune cell response as well as the impact on tumor growth at nontarget sites was evaluated in the Renca–CRL-2947 following LSAM-DTX injection. Tumors treated with IT LSAM-DTX had greater levels of CD4⁺ (Fig. 3b), CD8⁺ (Fig. 3c), and Treg cells (Fig. 3d) in their peripheral circulation compared to IT Vehicle. Increases in CD4⁺, CD8⁺, and Treg populations following IT LSAM-DTX treatment suggest that circulating immune effector cells may have contributed to growth inhibition of primary tumors as well as secondary untreated tumors. The increased immune-cell infiltration coupled with the tumor reduction/elimination suggests that IT LSAM-DTX was associated with a cytolytic secondary immune response [18].

COMBINATORIAL SYNERGISM

LSAM-DTX + Anti-CTLA-4

To characterize response of local tumors, metastatic disease, and immunomodulation, IT LSAM-DTX alone or in combination with IP anti-mCTLA-4 was evaluated in the 4T1-Luc (4T1) murine breast cancer orthotopic model [20]. Changes in tumor volume (TV) and

bioluminescence (BLI) of luciferase genomic insert were evaluated for tumor and metastatic response. IT LSAM-DTX treatments reduced TV compared to vehicle control; greatest reduction in BLI was seen in the thoracic area following combination treatment with IT LSAM-DTX + IP anti-mCTLA-4 (Fig. 4). All control and IP anti-mCTLA-4 and 9 of the 10 IT LSAM-DTX-treated animals developed metastasis by day 30 as determined by BLI signal. In the IT LSAM-DTX + IP anti-mCTLA-4 group, 40% of animals had no evidence of metastasis. A positive correlation was observed between reduced metastasis and TV reduction. The combination of IT LSAM-DTX + IP anti-mCTLA-4 was well tolerated as shown by animal weight gain and lack of adverse clinical findings [20].

Following IT LSAM-DTX, immune cell increases in tumor tissue were found, including density of CD4⁺ helper T cells, CD8⁺ T cells, B cells, natural killer T (NKT) cells, and dendritic cells (DCs). IT LSAM-DTX was associated with increases in T cell concentrations within the tumor along with increases in the peripheral blood (Fig. 5a). NKT cell concentrations also increased following IT LSAM-DTX + IP anti-mCTLA-4 therapy within the tumor and peripheral blood. NK cell concentrations increased in the tumor following IT LSAM-DTX or anti-mCTLA-4 monotreatment. The NK cell concentration increase is consistent with

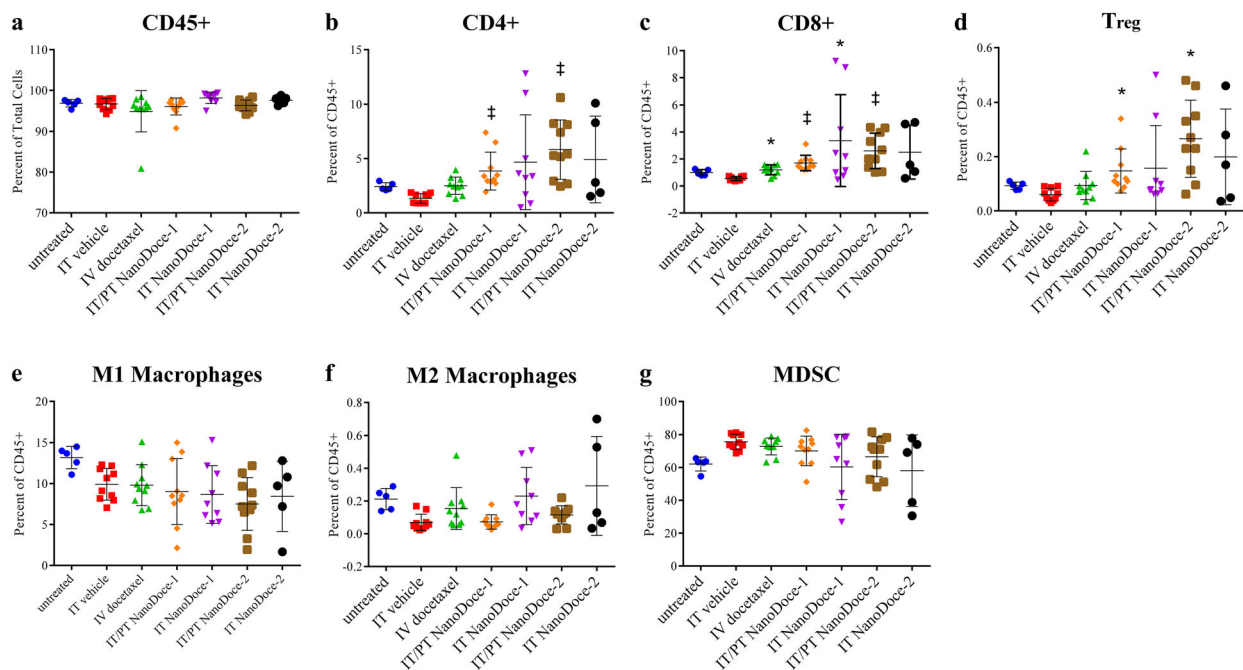


Fig. 3 Circulating lymphocytes detected in peripheral blood in animals with a single Renca tumor. **a** Similar levels of CD45⁺ leucocytes were detected in all samples. **b** IT LSAM-DTX, referred to as NanoDoce in the figure, treatments administered IT/PT (peritumorally) significantly increased circulating CD4⁺ T cells. **c** IV docetaxel and LSAM-DTX treatments significantly increased circulating CD8⁺ T cells. **d** IT/PT LSAM-DTX treatments resulted in increased circulating levels of Treg cells. Although there was a trend toward reduction following

IT LSAM-DTX treatment, no significant differences in circulating populations of macrophages (**e** M1 and **f** M2) or **g** myeloid-derived suppressor cells (MDSCs) were detected in docetaxel or LSAM-DTX treatments compared to IT vehicle. Graphs show individual animal samples with center lines representing means and error bars representing \pm Std. dev. Statistically significant differences vs. IT vehicle control are as follows: ‡ $p < 0.0001$; * $p < 0.001$. Adapted with permission from [18]

previous reports that NK cells arrive early in the TME after chemotherapy and, along with DCs, enable an effective T cell tumoricidal response [21–23]. Effectiveness of NK cells as immune effectors in treatment of solid tumors is typically limited by an inability to accumulate in the tumor [24]. In this study, the percentage of NK cells was greatest in blood after IT LSAM-DTX + IP anti-mCTLA-4 treatment. Also, combinatorial IT LSAM-DTX + IP anti-mCTLA-4 resulted in the highest DC levels in tumor and blood. The TV and BLI decreases after combinatorial therapy may, in part, be due to the local release of tumoricidal cytokines by the infiltrated NKT cells [25–27]. The hypothesis that IT LSAM-PTX and LSAM-DTX allow for continuous tumoricidal taxane levels which

enhances the adaptive immune system’s response to increased availability of tumor-associated antigens from continuous and prolonged tumor cell kill is supported by these observations [20].

LSAM-PTX + Anti-PD1

IT LSAM-PTX alone and in combination with IP anti-mPD-1 was evaluated for efficacy and pharmacodynamic properties in tumor and blood in a murine melanoma cell line (Clone M3 (Cloudsman S91)) implanted into the mammary fat pad of female mice [28]. The study consisted of five groups: untreated, IT vehicle control + IP isotype control, IT LSAM-PTX, IP anti-mPD-1, IT LSAM-PTX + IP anti-

mPD-1. Treatments were initiated on day 10 when primary TVs averaged 56.8 mm^3 (Fig. 6a). On day 20 (day of necropsy), both IT LSAM-PTX alone and IP anti-mPD-1 alone showed noticeable although not significant inhibitions of primary tumor growth compared to the corresponding vehicle-isotope control. When the IT LSAM-PTX + IP anti-mPD-1 combination was administered, there was a significant reduction in ex vivo tumor volume (Fig. 6b).

Flow cytometry of tumor-site tissues treated with IT LSAM-PTX + IP anti-mPD-1 showed reduced MDSC and DC levels in tumor tissues and increases in granulocytes and M2 macrophage concentrations compared to the IT vehicle + IP isotope control group. IT LSAM-PTX monotherapy resulted in increased concentrations from baseline of M2 macrophage. IP anti-mPD-1 monotherapy resulted in increases in macrophages and Treg cell levels in tumor tissue when compared to control treatment [28].

Flow cytometry of whole blood showed IT LSAM-PTX + IP anti-mPD-1 treatment resulted

in an increase in circulating granulocytes and a reduction in CD4^+ T cells, macrophages, and M1 macrophages (Fig. 7a). IT LSAM-PTX monotherapy decreased circulating macrophage levels compared to IP isotope control.

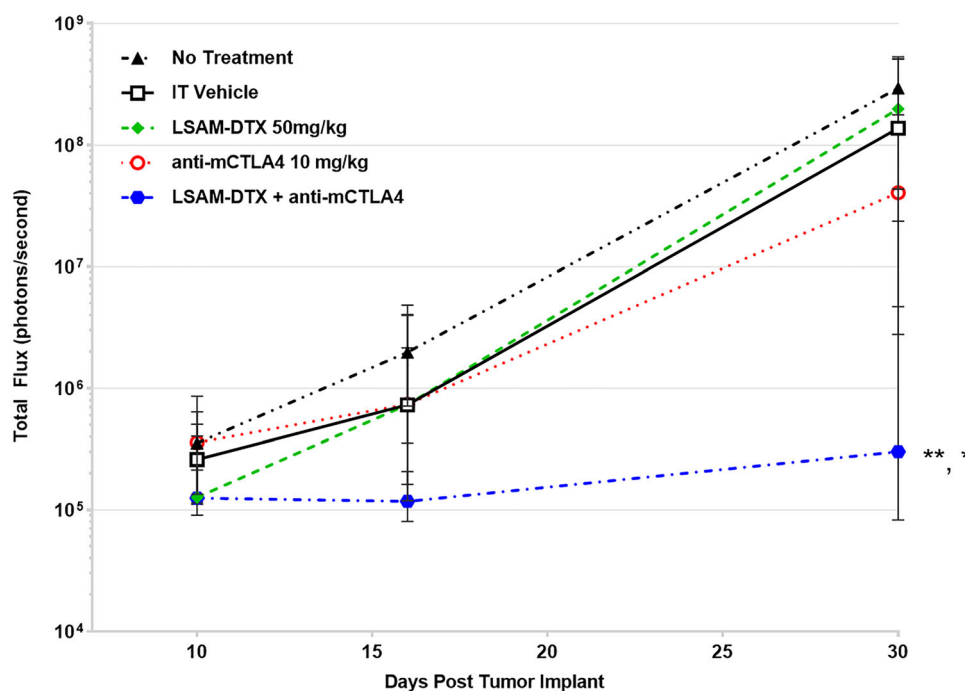
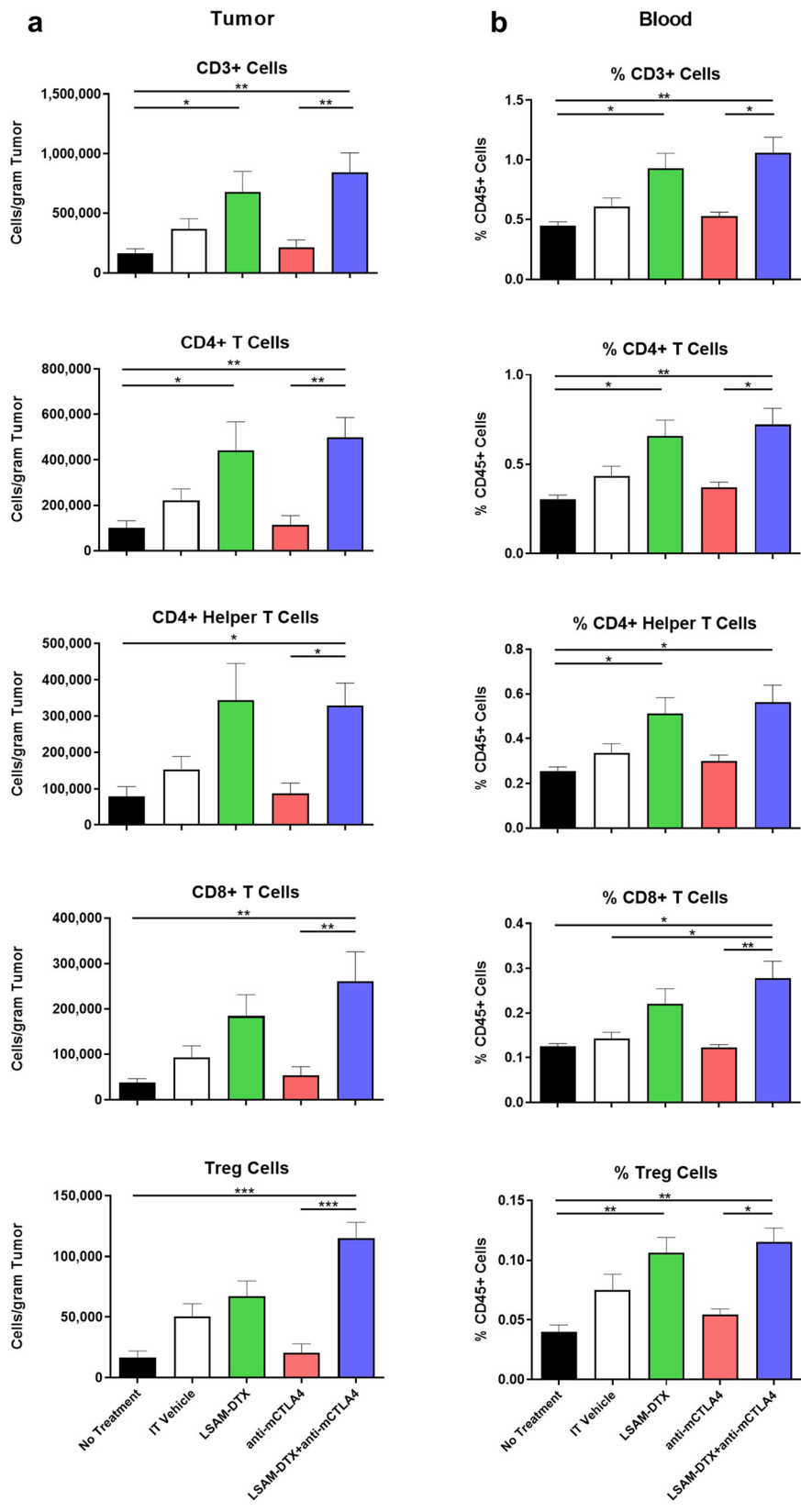


Fig. 4 Group median bioluminescence value (photons/second) \pm IQR at days 10, 16, and 30. $n = 10$ mice/group. Significance reported vs. no treatment controls, LSAM-

DTX monotherapy; $*p < 0.05$, $**p < 0.01$. Significance reported as $*p < 0.05$, $**p < 0.01$, $****p < 0.0001$. Adapted with permission from [15]



Interestingly, the only significant difference in immune cell populations in the lymph nodes was an increase in NK cell concentrations following treatment with the combination of IT LSAM-PTX + IP anti-mPD-1 (Fig. 7b). Importantly, administration of the combination regimen occurred without significant toxicity as shown by animal weight gain and lack of adverse clinical findings suggesting that IT LSAM-PTX combined with a checkpoint inhibitor may induce tumoricidal response greater than either therapy alone without added systemic toxicity [15].

CLINICAL EXPERIENCE WITH LSAM TAXANES

LSAM-PTX: Intraprostatic Injection of Localized Prostate Cancer

The safety of LSAM-PTX delivered via intraprostatic injection in subjects ($n = 16$) with localized adenocarcinoma of the prostate scheduled for prostatectomy 30 days later was evaluated [16] (NCT03077659). The phase 1 trial was a single-arm, open-label, 3 + 3 dose-escalation design (6, 10, 15 mg/mL) with additional enrollment at the high dose. LSAM-PTX was administered under magnetic resonance imaging-transrectal ultrasound fusion guidance into the prostate lobe containing the dominant lesion in a volume no greater than 20% of the lobe. Three subjects were enrolled in the 6 mg/mL, three in the 10 mg/mL, and ten in the 15 mg/mL dose groups, respectively. There were no serious adverse events, dose limiting toxicities (DLTs), clinical prostatitis, or subject discontinuation from the study reported as a result of treatment emergent adverse events (TEAEs). All TEAEs were considered mild or moderate in severity, except for one event that was severe in nature but determined to be unrelated to LSAM-PTX. No systemic DLTs or toxicities typically attributable to paclitaxel such as neutropenia, thrombocytopenia, peripheral neuropathy, and hypersensitivity reactions were reported.

Plasma paclitaxel concentrations for the 10 mg/mL and 15 mg/mL cohorts were larger than the 6 mg/mL cohort. The mean plasma

concentration–time profiles converged about 1 week after injection for all three cohorts and followed the same profile for the remainder of the study. By day 29, the plasma concentration of paclitaxel dropped below the lower limit of quantitation (LLOQ; 25 pg/mL) in only two subjects, and all remained above the LLOQ at day 29 in the 15 mg/mL cohort. The highest plasma concentrations, between 19 and 20 ng/mL of paclitaxel, were recorded at the earliest sample (the 1-h post-injection timepoint). In contrast, significant concentrations of paclitaxel were detected in all prostate tissue samples obtained during prostatectomy (except for one sample in the 6 mg/mL cohort), in pelvic lymph nodes of nine subjects (one, two, and six of subjects in the 6, 10, and 15 mg/mL cohorts, respectively), and in most ejaculate samples.

Tumor response was variable across the three concentrations of LSAM-PTX over 4 weeks of exposure, which may have been due to the small size of the study, short study duration, lack of complete coverage of the tumor with drug, and/or the slow rate of prostate cancer cell mitosis. The prostate volumes generally increased between the time of injection and prostatectomy, possibly owing to the injection volumes or immune response generated by IT LSAM-PTX. Eleven of 16 subjects had stable or reduced proportions of cancer in their prostate tumor biopsy. Of these 11 subjects, six showed reductions in proportion of tissue identified as adenocarcinoma, while five subjects showed no change. The sum of the volumes of the dominant lesions at screening and day 29 were 11.45 cm³ and 8.54 cm³, respectively, a 25.4% overall TV reduction approximately 30 days after IT LSAM-PTX. PSA density was reduced from screening to day 29 in all cohorts; in the 15 mg/mL cohort a 34% reduction was observed. Remarkably, standard immunohistochemistry of the prostate tumor sections revealed immune effector cell infiltration into all the prostates in the areas of LSAM-PTX injection. Ma et al. [29] reported that IV docetaxel enhances immune cell infiltration and immune checkpoint inhibitor response in human prostate cancer.

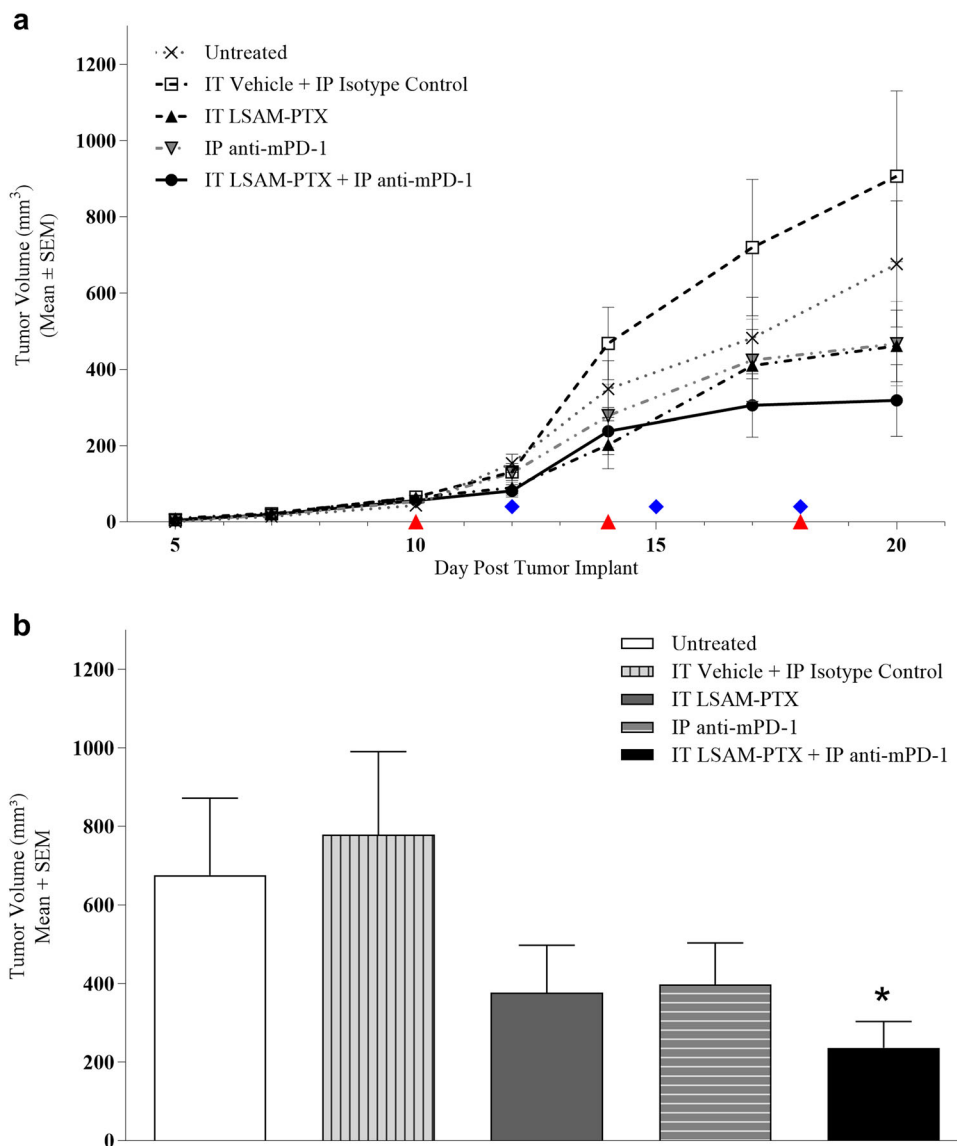
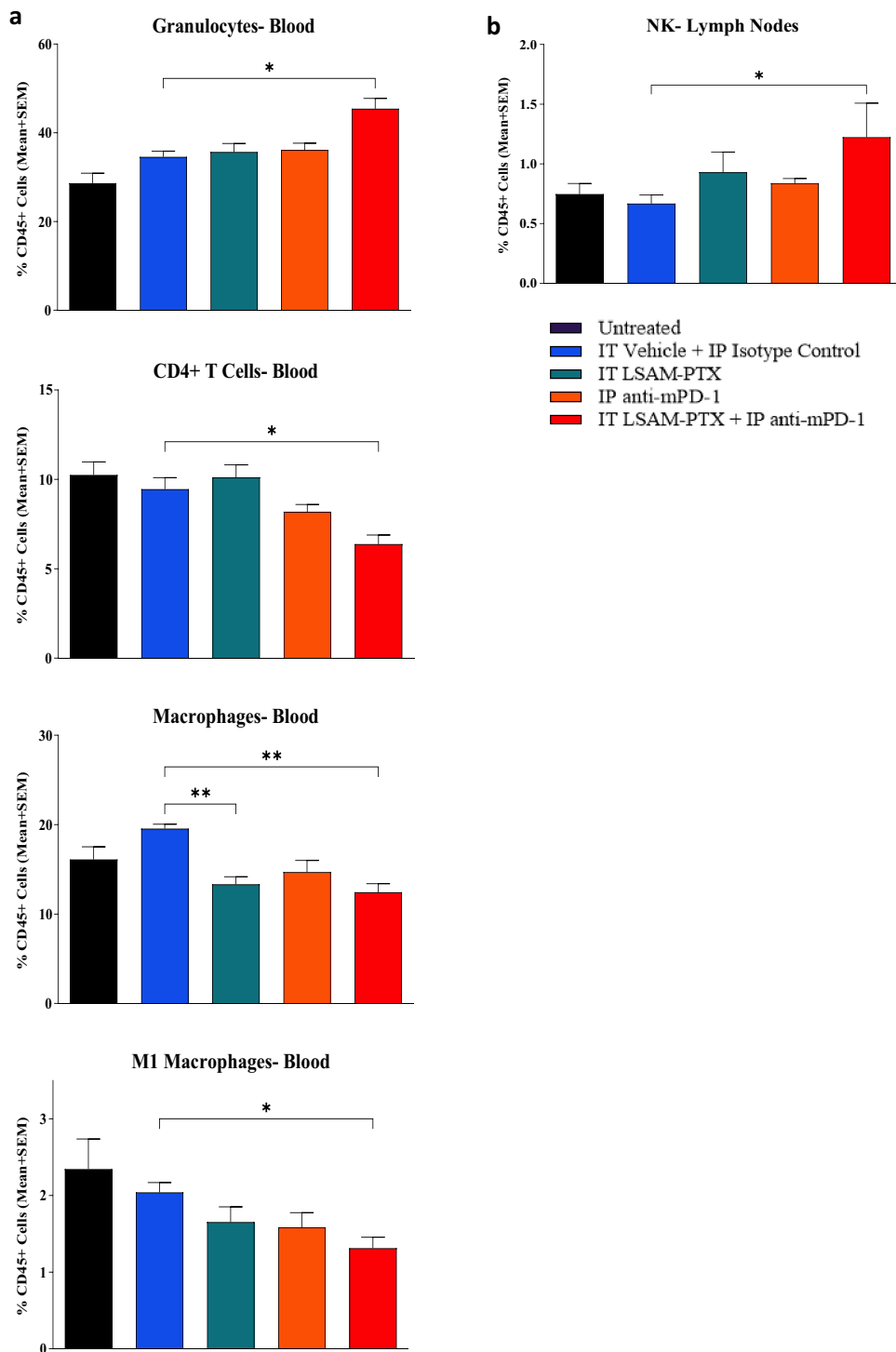


Fig. 6 a Clone M3 primary tumor volumes. Tumors were implanted on day 0. Ten days later, when mean TV = 56.8 mm³, animals were randomized to five groups. IT LSAM-PTX (approx. 60 mg/kg) was administered on days 10, 14, and 18; IP anti-mPD-1 (10 mg/kg) was administered on days 12, 15, and 18. Combination IT LSAM-PTX + IP anti-mPD-1 was administered at the same dose and schedules as the single treatments. IT vehicle + IP isotype control treatments were administered on the same schedule as the combination treatments. Untreated animals exhibited tumor growth consistent with previous studies. There were *n* = 8 animals/group throughout study with exception of the IT LSAM-PTX

group with *n* = 7 animals starting at day 10 and the IT vehicle + IP isotype control group with *n* = 7 animals starting at day 19; no other animals exited prior to day 20. Data are group mean tumor volumes ± SEM. Treatment days are indicated as red triangles (LSAM-PTX) or blue diamonds (anti-mPD-1). **b** Clone M3 mean tumor volumes (mm³) measured on day 20 were significantly reduced in animals administered combination IT LSAM-PTX + IP anti-mPD-1 treatment compared to IT vehicle + IP isotype control animals. There were no other statistically significant differences between groups. Data are group mean tumor volumes + SEM; **p* < 0.05. Adapted with permission from [28]



◀**Fig. 7** Changes in immune cell populations in mice implanted with Clone M3 tumors. **a** Whole blood collected at end of study found changes in granulocytes, CD4⁺ T cells, macrophages and M1 macrophages. **b** Axial and inguinal lymph nodes collected at end of study found significant increases in NK cells. Samples were collected on day 20 in animals left untreated (black bar) or administered 3 cycles of IT vehicle + IP isotype control (blue bar), IT LSAM-PTX (approx. 60 mg/kg; green bar), IP anti-mPD-1 (10 mg/kg; orange bar), and or IT LSAM + IP anti-mPD-1 combination treatment (approx. 60 mg/kg; red bar). For each population, data are displayed as group mean of %CD45⁺ cells + SEM. Comparison to IT vehicle + IP isotype control performed using Kruskal–Wallis and Dunn’s multiple comparisons tests; **p* < 0.05; ***p* < 0.01; ****p* < 0.001. Adapted with permission from [28]

LSAM-DTX: Intramural Injection and Intravesical Instillations for Treatment of Bladder Cancer

Safety, preliminary efficacy, and immune effects of LSAM-DTX injection into the tumor site after transurethral resection of bladder tumors (TURBT) followed by intravesical instillations of LSAM-DTX were evaluated in subjects (*n* = 19) with high-risk non-muscle invasive bladder cancer (hrNMIBC) [30] (NCT03636256). The trial was a single-arm, open-label, 3 + 3 dose-escalation design of intramural injection of the resection site (0.75, 1.5, 2.5, or 3.75 mg/mL; up to 4 mL) and intravesical instillation (50 mg or 75 mg in 25 mL) with additional enrollment at the highest doses of both injection and intravesical treatments. After confirmation of resection site healing of at least 4 weeks post-TURBT and intramural LSAM-DTX injection, subjects received intravesical instillations of LSAM-DTX on a 6-week induction and 3-week maintenance schedule. In the three lowest dose cohorts the median recurrence free survival (RFS) was 5.4 months (*n* = 10; median follow-up 8.6 months). In subjects receiving 3.75 mg/mL intramural injection, the median RFS was increased to 12.2 months (*n* = 9; median follow-up 12.4 months). Of the nine subjects who received the three highest doses of LSAM-DTX, RFS was sustained in 9 (100%), 7 (78%), and 4

(50%) at 3, 6, and 12 months, respectively, with one subject declining 12-month follow-up. Systemic docetaxel exposure was negligible; only two samples in two subjects had docetaxel concentrations above the LLOQ (10 ng/mL; 11.6 ng/mL at 4 h after injection and instillate, and 10.3 ng/mL at 1 h after injection and instillate).

Bladder biopsies of resection site after LSAM-DTX treatment showed an increase in concentrations of immune effector cells including T cells and NK cells. These increases in immune cell levels in the tumor site biopsy were accompanied by elevations in PD-1, PD-L1, and CTLA-4 immune checkpoint inhibitor expression (Fig. 8). Checkpoint expression increased in all evaluated cell types, including T cells, macrophages, and PanCK⁺ cells, suggesting local treatment with LSAM-DTX followed by checkpoint inhibitors could extend RFS [31]. In two subjects with no recurrence at 12 months, antitumor immunophenotypes were more pronounced which suggests that improvement in clinical outcome may be due to increased immunogenicity of the TME (Fig. 9). These subjects were both BCG-naïve without prior TURBT, suggesting that changes in immune cell constitution and distribution in the tumor, as well as clinical response, were a result of LSAM-DTX treatment [30].

Previous reports correlating immune cell levels in bladder tissue to clinical course of bladder cancer found that higher concentrations of cytotoxic T cells and NK cells, like those reported in subjects treated with LSAM-DTX, are predictive of improved overall survival (OS), progression free survival, and increased expression of immune checkpoint targets such as CTLA-4 [32]. Based on tumoricidal synergy with associated changes in tumor infiltration of effector cells reported after IT LSAM-DTX followed by systemic anti-CTLA-4 in the 4T1 study [20], LSAM-DTX administration to TURBT resection sites followed by intravesical or intravenous anti-CTLA-4 may extend RFS in patients with hrNMIBC [15].

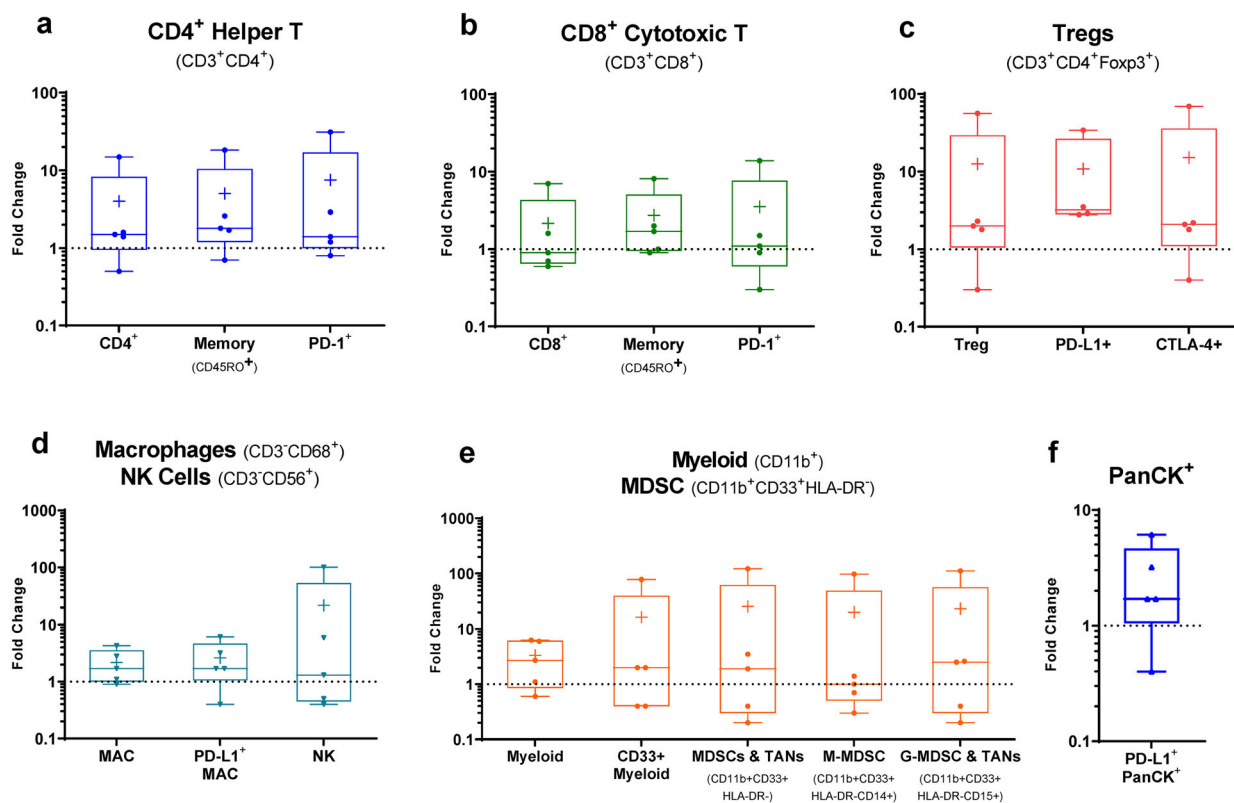


Fig. 8 Changes in immune cell density in NMIBC. Subjects' fold-change in immune cell densities (cells/mm²) from biopsies collected before and after LSAM-DTX therapy as determined by multiplex immunofluorescence (mIF). Boxplots show min. to max. fold-changes (extremes), per subject data (dots), mean (+), and median (line) for $n = 5$ subjects analyzed. Cell types are identified using marker co-expression over an average of 24 regions of interest (ROI; range 7–37) within the TME per slide. Region of interest (ROI) selected by a pathologist blinded

to treatment status on a hematoxylin and eosin-stained slide. Cell type density is the total number of cells counted divided by the total area (sum of all ROI areas) per slide. In cases where the pre-LSAM-DTX cell density was 0 cells/mm², no data is reported and $n < 5$. **a** CD4⁺ helper T cells. **b** CD8⁺ cytotoxic T cells. **c** Treg cells. **d** Macrophage (MAC) and NK cells. **e** Myeloid and MDSC cells; MDSC and tumor associated neutrophils (TANs). **f** PanCK⁺ PD-L1⁺. Adapted with permission from [31] and [15]

LSAM-PTX: Intratumoral Treatment of Locally Advanced Pancreatic Cancer (LAPC)

Safety, tolerability, and tumor response to IT LSAM-PTX given as a neoadjuvant to subjects with LAPC (tumor 1.5–6 cm), confirmed as unresectable by each clinical site prior to enrollment, were evaluated in a single-arm, open-label trial using endoscopic ultrasound-fine needle injection directly into the tumor [33] (NCT03077685). The first phase of the study followed a traditional 3 + 3 dose-escalation design for a single injection of three

concentrations of IT LSAM-PTX (6, 10, and 15 mg/mL), up to 20% of the calculated tumor volume (with a maximum injection volume of 5 mL per subject). The dose escalation cohort ($n = 10$) was followed by an initial dose-expansion cohort ($n = 25$) of two monthly injections. After LSAM-PTX treatments were initiated, subjects underwent a 6-month follow-up to assess disease control rate (DCR) and multiplex immunofluorescence (mIF) of available tissue biopsies or tumor resections to evaluate immune response.

No DLTs or events of pancreatitis were reported. Plasma paclitaxel levels were

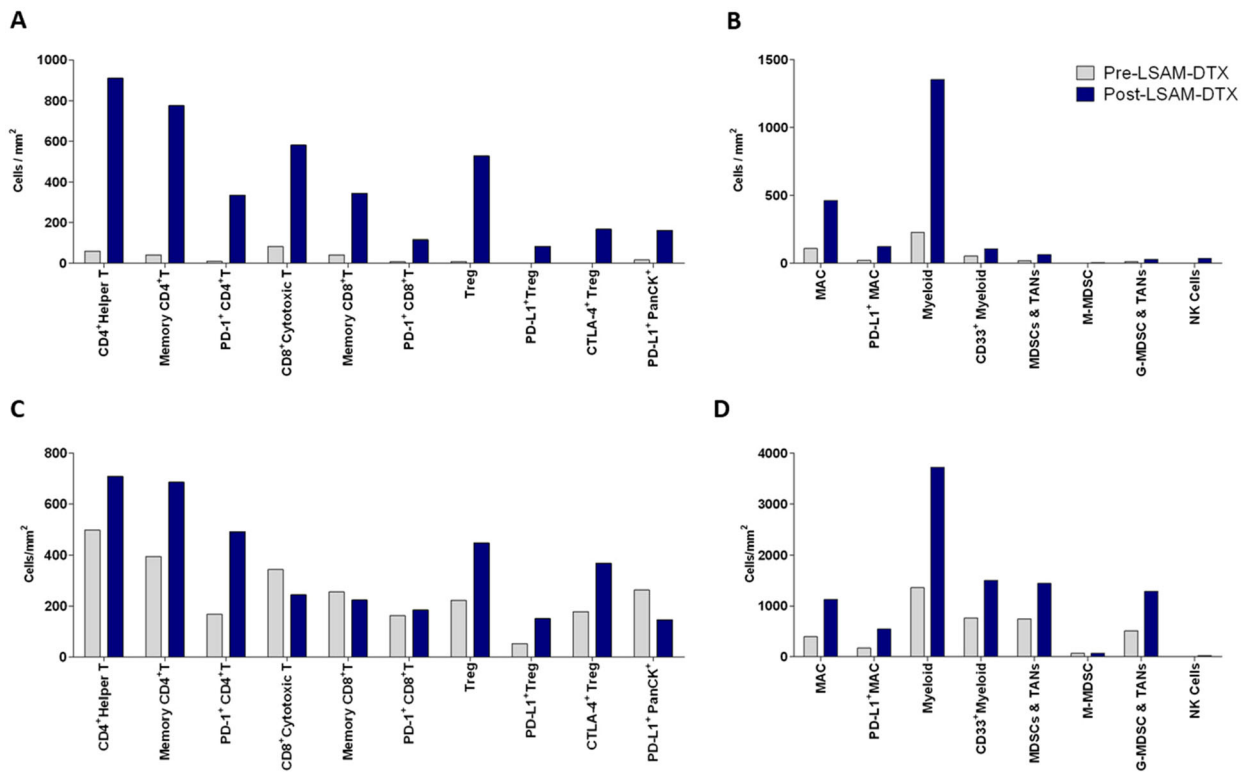


Fig. 9 Multiplex immunofluorescence data from bladder biopsies collected pre- and post-LSAM-DTX therapy in the only 2 BCG-naïve high-risk NMIBC subjects who had no TURBT procedures prior to day 1. Both subjects had complete response (CR) at 12 months and showed increases in post-LSAM-DTX density of adaptive and innate immune cells including increases in the immune checkpoint inhibitor targets PD-1 (increased on CD4⁺ helper T, CD8⁺ cytotoxic T), PD-L1 (increased on Treg, macrophages, and PanCK⁺ cells), and CTLA-4 (increased on Treg) compared to pre-LSAM-DTX (collected at TURBT). Cell types are identified using marker (CD11b, CD14, CD15, CD3, CD4, CD8, CD20, CD33, CD45RO, CD56, CD68, HLA-DR, FOXP3, CTLA4, PD-1, PD-L1, and Pan-cytokeratin (PanCK)) co-expression over regions of interest (ROI) within the tumor microenvironment per slide. ROI was selected by a pathologist blinded to treatment status on a hematoxylin and eosin-stained slide. Cell type density is the total number of cells counted divided by the total area (sum of all ROI areas) per slide. **a** Widespread increases in adaptive

immune cells, including increased density of effector T cells as well as increases in PD-L1⁺ PanCK⁺ cells in biopsy collected after LSAM-DTX treatment completion (end of study (EOS) at 5.3 months post-TURBT) compared to pre-treatment biopsy is seen in the first subject. **b** Changes in innate immunity in the first subject include increased density of MAC and myeloid cells within the tumor microenvironment in biopsy collected at EOS. **c** Following LSAM-DTX treatment, a second subject demonstrates increase in components of adaptive immunity within the tumor microenvironment in biopsy collected 4.0 months post-TURBT; specifically increases in CD4⁺ T cells (including memory and PD-1⁺) and Treg cells (including PD-L1⁺ and CTLA-4⁺). **d** Changes in innate immunity in tumor microenvironment of a second subject following LSAM-DTX therapy include increases in density of MAC, myeloid (including CD33⁺), MDSC, G-MDSCs, and TANs. Adapted with permission from [30] and [15]

negligible and routine laboratory blood tests unremarkable. Interestingly, investigators stated that subsequent LSAM-PTX injections were associated with a reduction in resistance to

injection pressure consistent with drug-induced alteration of the tumor's interstitial spaces and density [33]. In 8 of 22 (36%) evaluable subjects in the two-injection cohort, previously

unresectable tumors were downstaged to resectable after IT LSAM-PTX and standard of care chemotherapy; 5 of 6 were resected with R0 margins (83%). Pathology reported complete or significant tumor necrosis in all specimens. DCR at 6 months was 94% and the median OS from diagnosis was 19.7 months (median follow-up 14.3 months). The OS from diagnosis for non-resected and resected groups was 18.9 and 35.2 months, respectively [33].

As the TME of LAPC is well known to be resistant to immune effector cell infiltration following IV chemotherapy, it is often referred to as the classic “cold tumor” [34–37]. Tumor-site tissues from six subjects were available from pre-treatment biopsies and resected tumor following IT LSAM-PTX for immunophenotyping using mIF (Fig. 10). Resected tumor contained increases in helper T cell densities compared to the tumor-site biopsy tissue prior to IT LSAM-PTX therapy. Trends toward increases in CD3⁺CD4⁺PD-1⁺ helper T cell density (5.6-fold increase; Fig. 10a) and CD3⁺CD8⁺ cytotoxic T cell density were also found in resected tumors. Treg cell (CD3⁺CD4⁺Foxp3⁺) concentrations were minimally changed between pre-LSAM-PTX treatment and resection. A significant 4.8-fold increase in density of NK cells (CD3⁻CD56⁺) was present in resected tissue (Fig. 10d). Macrophage (CD3⁻CD68⁺) concentrations were increased in both intraepithelial and stromal regions (Fig. 10e). CD11b⁺ myeloid cell levels were decreased in resected samples, including myeloid-derived suppressor cells (M-MDSC) and G-MDSC (Fig. 10f). Increases in effector T cells, antitumor NK cells, and macrophages combined with decreases in MDSC in samples from resected subjects suggest that IT LSAM-PTX treatment results in an antitumor immunophenotypic cell infiltration into the tumor. Interestingly, there was an increase in expression of PD-L1⁺ (2.4-fold) and CTLA-4⁺ Treg cells (1.9-fold) in tumor tissue resected after IT LSAM-PTX (Fig. 10c) that was reminiscent of similar changes following LSAM-DTX tumor site injections in treated patients with hrNMIBC (Fig. 8). On the basis of these findings, prior to and following treatment, immunophenotyping of the tumor as well as flow cytometric evaluation of peripheral blood

should be performed in future trials with IT LSAM-PTX combined with checkpoint inhibitors [33].

DISCUSSION

Priming the immune system with IV chemotherapy prior to immunotherapy has been used to reinstate or enhance immunosurveillance [38–40]. Barriers of taxane access to the TME when administered IV, including high interstitial fluid pressure, growth-induced solid stress, and stromal matrix, exceed the modest increase in enhanced capillary permeability and hydraulic conductivity associated with tumor-recruited neovascularization [41, 42]. Direct injection of LSAM-PTX or LSAM-DTX into primary carcinomas catalyzes a cascade of events involving both antimitotic and immune-mediated effects that enhance tumor kill. In xenograft studies in immunocompromised animals, as well as in orthotopic studies in the immune intact models summarized here, greater tumor volume reduction was achieved following IT LSAM-PTX or LSAM-DTX compared to the taxane given IV along with increased concentrations of immune cells in the peripheral blood and tumor. When LSAM-PTX or LSAM-DTX was injected directly into the tumor, their retention exposed replicating tumor cells to continuous tumoricidal drug levels for weeks [16]. This ongoing cell death may affect the immune system by (1) increasing release of tumor specific antigens, (2) decreasing the number of immunosuppressive cells, and (3) attracting phagocytic cells to remove tumor cell debris.

Systemic toxicity of combinatorial regimens including chemotherapy and immunotherapy can limit therapeutic benefit because of their additive toxicities requiring reductions in dose and/or “treatment holidays” during a prescribed course of therapy. The nontargeted nature of IV chemotherapy exposes the entire body to potentially toxic levels of cytotoxic drug often requiring dose and administration frequency (dose density) adjustments in response to patient tolerance. In clinical trials of LSAM-DTX to treat hrNMIBC and IT LSAM-PTX to treat LAPC and localized prostate cancer, taxane

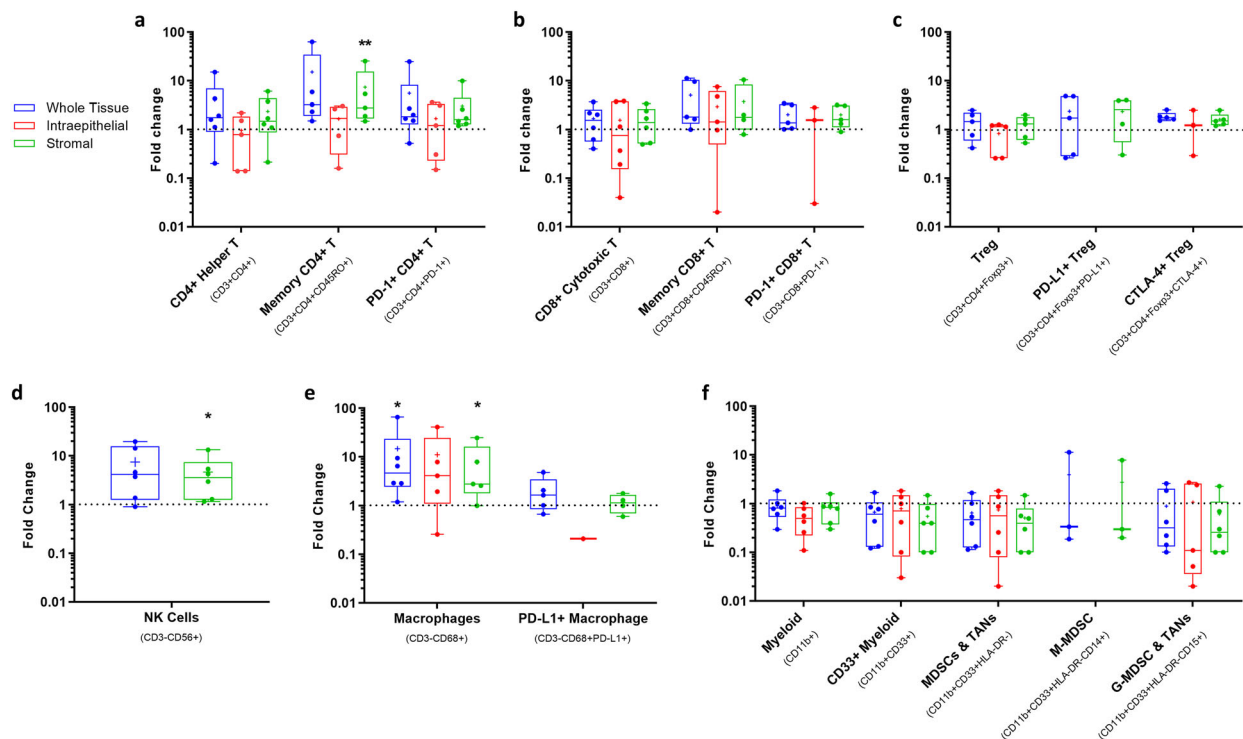


Fig. 10 Fold-change in density (cells/mm³) of immune cells as determined by multiplex immunofluorescence (mIF) of pancreatic tumor tissues collected pre-LSAM-PTX injection and at resection. Box and whisker plots display range of density fold-changes with median and mean plotted as a line and +, respectively, and individual subject results overlaid. Density is determined for the entire sample (whole tissue; blue plots), for the intraepithelial region defined by cells in contact with PanCK⁺ tumor cells (intraepithelial, red plots), or immune cells found outside of direct contact with PanCK⁺ tumor cells (stromal; green plots) and only plotted if both pre-injection and resection cell densities were > 0 mm³. **a** CD4⁺ helper T cell densities including CD45RO⁺ memory and PD-1⁺ cells. **b** CD8⁺ cytotoxic T cell

densities including CD45RO⁺ memory and PD-1⁺ cells. **c** Treg cell densities including PD-L1⁺ and CTLA-4⁺ cells. **d** Natural killer (NK) cells for whole tissue and stromal regions; intraepithelial region is not included because of cross-reactivity between CD56⁺ and PanCK⁺ cells. **e** Macrophage cell densities including PD-L1⁺ cells. **f** Myeloid, myeloid-derived suppressor cells (MDSC), and TAN cell densities including granulocytic myeloid-derived suppressor cells (G-MDSC) and monocytic myeloid-derived suppressor cells (M-MDSC). Significance values determined by paired *t* test (parametric) with 95% confidence levels are reported as **p* < 0.05 or ***p* < 0.01. Adapted with permission from [33]

plasma levels were negligible and treatments were well tolerated by study subjects who did not experience systemic toxicities typically associated with IV taxanes. In preclinical studies, following a single IT administration of LSAM-DTX or LSAM-PTX, docetaxel and paclitaxel were found in the tumor at levels much greater and for longer periods of time than achievable by IV chemotherapy. In addition, high taxane levels in the tumor did not result in immunosuppression commonly associated with

IV chemotherapy. Importantly, local administration of LSAM-PTX or LSAM-DTX may synergize with immunotherapy without exposing nontarget organs to additional toxicity [15].

Tumor heterogeneity and emergence of drug resistance are major contributors to chemotherapy failure [36, 43–45]. In addition to genetic factors, heterogeneity from stroma, fibroblast recruitment, immune cell migration, matrix remodeling, and tumor-specific vasculature create nongenetic variability in the tumor

landscape [41, 43, 46]. Although intra-arterial endovascular infusion of LSAM-PTX or LSAM-DTX could potentially facilitate intratumoral drug distribution, the blood–tumor barrier reduces tumoricidal response in regions of the tumor distal to vasculature [47–49]. For example, in subcutaneous PC-3 prostate cancer xenografts, doxorubicin concentrations following IV infusion decrease exponentially with increasing distance from blood vessels and failed to kill cancer cells [50]. Molecular biomarkers including driver mutations within tumor cells, plasma membranes enveloping cell-level biomarkers, blood vessel endothelium, and separating tissue-level biomarkers within the TME are less likely to create neoantigens available to immune surveillance in tumor not exposed to tumoricidal concentrations of drug [48, 51, 52]. Taken together, these observations suggest that multiple routes of drug administration to solid tumors may be required to maximize primary tumor eradication and reduce metastatic disease [44, 53, 54].

Mechanism of Action

The primary cytotoxic mechanism of taxanes is inhibition of tubulin depolymerization, suspending mitosis in the G2/M phase interfering with cell division which can lead to apoptotic and necroptotic tumor cell death [55]. Necroptosis is a drug- and dose-dependent mechanism of tumor cell destruction achieved by continuous exposure to high chemotherapy levels. Necroptosis is characterized by loss of tumor cell membrane integrity, exposing tumor-specific antigens to immune surveillance which can stimulate a robust response of the adaptive immune system to tumor-specific antigens [16, 56–58]. Immunogenicity requires that tumor cells provide adequate levels of antigens and that the tumor cells effectively present antigens in a form that leads to immune activation instead of immune tolerance which can occur when antigen is presented intermittently, in low quantities, and with progressive modifications [59]. Chemotherapy-induced tumor cell necrosis may induce both pro-inflammatory and immunogenic responses [60–62]. Paclitaxel-

induced immunomodulation involves many aspects of immune function, including lymphocyte recruitment and activation, antigen processing and presentation, as well as production of immunoenhancing cytokines, including interleukin-12 (IL-12), IFN γ , and tumor necrosis factor- α (TNF α), resulting in enhancement of the antitumor activity of immunotherapies [63–67]. Paclitaxel was shown to increase concentrations of tumor-infiltrating lymphocytes [39] and activate CD8⁺ T cells while reducing immunosuppressive cells, such as regulatory T cells leading to immunogenic cell death [63, 65, 66, 68–70]. Docetaxel was reported to favorably mediate the anticancer response of macrophages, CD8⁺ T cells, B cells, and NK cells. Increases in immune cell density in the tumor following IT LSAM-PTX or LSAM-DTX supports the hypothesis that local LSAM administration initiates tumor cell death by both direct cytotoxic effects and recruitment of effector immune cells into the tumor [15, 16]. Response of carcinomas to prolonged and continuous exposure to tumoricidal levels of LSAM-PTX or LSAM-DTX may involve at least two different mechanisms. First, direct tumor kill by taxane-induced suspension of mitosis followed by cell disruption, making neoantigens available inducing antigen spread within the TME. Second, these conditions stimulate immune effector cell infiltration to further the local tumoricidal response [16]. This hypothesis warrants additional investigation by measurement of cytokine production as well as T cell exhaustion [71]. The prolonged tumor residence of IT LSAM-PTX and LSAM-DTX may enhance permeability of the tumor's stromal matrix facilitating distribution and availability of neoantigens and drug throughout the tumor. LSAM-PTX- and LSAM-DTX-induced cell death appears to be a continuum between apoptosis and necroptosis, which depends on drug concentration and duration of tumor cell exposure [57, 63, 65]. As a result, continuous presence of high taxane levels in the tumor creates a more favorable immune microenvironment for immunotherapy.

Synergism with Checkpoint Inhibitors

Use of immune checkpoint inhibitors in combination with chemotherapy, radiation, or oncolytic viruses has shown added benefit in preclinical and clinical studies [29, 72–81]. This is evidenced by the US Food and Drug Administration's (FDA) initial approval of atezolizumab, a monoclonal antibody targeting PD-L1, combined with chemotherapy for the treatment of adults with PD-L1-positive, advanced triple-negative breast cancer [81] as well as other recent combinatorial drug approvals. Multiple ongoing clinical trials will likely expand FDA approval of combinatorial therapies in the future [82–87]. However, clinical results from trials evaluating systemic combinations of chemotherapy and immunotherapy have often been disappointing [34, 61, 88, 89]. Reduced synergism with systemic therapies may be due, in part, to depletion of lymphocytes from IV chemotherapy-related bone marrow suppression [90]. Failed immune responses aid in the selection of cancer cell clones that are less likely to undergo immune-mediated destruction [91]. Selection pressure and tumor cell replication between cycles of IV chemotherapy allow for mutational mitosis that creates drug-resistant cell lines and a tumor survival advantage which may be mitigated by continuous exposure of the tumor cells to tumoricidal drug levels.

Efficacy of immune therapy may be improved by administration of locally administered LSAM-PTX or LSAM-DTX to enhance the availability and antigenicity of tumor cells and their fragments thereby increasing tumor recognition and eradication by immune effector cells. Treatment of the primary tumor with LSAM-PTX or LSAM-DTX may also enhance response to immunotherapy of the primary tumor and metastatic disease by increasing the number of immune cells expressing checkpoints. Increases in checkpoint expression by immune cells were found following LSAM-PTX and LSAM-DTX treatment of tumors/tumor resection sites in subjects with LAPC and hrNMIBC, respectively [30, 33]. Potential synergistic benefits from combinatorial IT LSAM-PTX or LSAM-DTX and immune checkpoint

inhibitor therapy may be explained, in part, by the finding that shortly after chemotherapy, checkpoint expression tends to increase [88, 92, 93].

Enhanced Immune Response in the Tumor and Peripheral Blood

An increase of effector immune cell concentrations in tumors enhances immunogenic cell death while increasing the efficacy of immune checkpoint inhibitors [1, 94–96]. Following IT LSAM-PTX or LSAM-DTX treatment of solid carcinomas, immune effector cell concentrations from both the innate and adaptive immune systems were increased in the tumor and peripheral blood in preclinical studies [18, 20, 28] and clinical trials [30, 33]. T lymphocytes, NKT cells, and NK cells represent the major cytotoxic cells involved in tumor cell death. Elevation in peripheral blood concentrations of effector T and NK cells and reductions in immune suppressor cell levels occurred following IT LSAM-DTX in preclinical studies. Following stimulation of immune cell infiltration, NK cells typically arrive early in the TME and, together with DC, facilitate T cell-mediated tumoricidal response [21–23]. In the TME, NK cells often do not accumulate in the tumor after IV treatments [24]. Following treatment of 4T1-Luc subcutaneous tumors, the combination of IT LSAM-DTX + IP anti-mCTLA-4 decreased both TV and thoracic metastasis as well as induced increases in NK, T, and NKT cell levels in the tumor and peripheral blood [15]. In addition, increases in NK cells were also seen in clinical trials after administration of LSAM-DTX and LSAM-PTX [30, 33].

CONCLUSION

Since the initial observation that treatment of carcinomas with LSAM-PTX in a Cal-U-3 lung tumor stimulated tumor infiltrates of immune cells [97], substantial reductions in tumor volume and increased immune cell infiltrates into solid tumors have been observed in preclinical studies and clinical trials evaluating locally administered LSAM-PTX and LSAM-DTX, as

summarized here. IT LSAM-PTX- and LSAM-DTX-induced tumoricidal responses are accompanied by favorable immunomodulation in the tumor and/or peripheral blood, including increased immune effector cells from both innate and adaptive systems, increased checkpoint expression, and decreased immune suppressor cells. Development of LSAM-PTX and LSAM-DTX together with advances in minimally invasive procedures for local drug delivery allow for immune priming of solid tumors virtually anywhere in the body [8] to increase response to immune checkpoint inhibitors without stacking toxicity. Long-term safety studies have not yet been performed. Expansion of combinatorial trials to include locally administered LSAM-PTX or LSAM-DTX as adjunctive therapy followed by immunotherapy to enhance primary and systemic tumor kill deserves further investigation in clinical trials.

ACKNOWLEDGEMENTS

The authors would like to thank Emily Williams, Karan Dewnani, and Laura diZerega for their editorial assistance in the preparation of this review. We would also like to thank the participants of the clinical trials included in this review.

Author Contributions. Gere S. diZerega, Holly A. Maulhardt, and Shelagh J. Verco contributed to the study conception and design. Material preparation, data collection, and analysis were performed by Gere S. diZerega, Holly A. Maulhardt, Shelagh J. Verco, Michael J. Baltezer, and Alyson Marin. The first draft of the manuscript was written/revised by Gere S. diZerega, Samantha A. Mauro, and Alyson M. Marin. All authors commented on previous versions of the manuscript. All authors read and approved the final manuscript.

Funding. This research was funded by NanOlogy, LLC. The Rapid service fee was funded by NanOlogy, LLC.

Data Availability. The datasets generated during and/or analyzed during the current

study are available from the corresponding author on reasonable request.

Declarations

Conflict of Interest. Alyson M. Marin, Shelagh J. Verco, Samantha A. Mauro, and Holly A. Maulhardt report being full-time employees of US Biotest Inc; Gere S. diZerega and Marc A. Iacobucci report holding consultant/advisory roles, having stock ownership or receiving funding from NanOlogy, LLC.

Ethical Approval. All institutional and national guidelines for the care and use of laboratory animals were followed. Investigational review boards for all participating clinical sites provided approval for protocol and informed consents for subjects in accordance with the Code of Federal Regulations and local requirements. All procedures followed were in accordance with the ethical standards of the responsible committee on human experimentation (institutional and national) and with the Helsinki Declaration of 1975, as revised in 2000 (5). Informed consent was obtained from all patients for being included in the study.

Open Access. This article is licensed under a Creative Commons Attribution-NonCommercial 4.0 International License, which permits any non-commercial use, sharing, adaptation, distribution and reproduction in any medium or format, as long as you give appropriate credit to the original author(s) and the source, provide a link to the Creative Commons licence, and indicate if changes were made. The images or other third party material in this article are included in the article's Creative Commons licence, unless indicated otherwise in a credit line to the material. If material is not included in the article's Creative Commons licence and your intended use is not permitted by statutory regulation or exceeds the permitted use, you will need to obtain permission directly from the copyright holder. To view a copy of this licence, visit <http://creativecommons.org/licenses/by-nc/4.0/>.

REFERENCES

1. van den Ende T, van den Boorn HG, Hoonhout NM, et al. Priming the tumor immune microenvironment with chemo(radio)therapy: a systematic review across tumor types. *Biochim Biophys Acta Rev Cancer*. 2020;1874(1):188386. <https://doi.org/10.1016/j.bbcan.2020.188386>.
2. Wei SC, Duffy CR, Allison JP. Fundamental mechanisms of immune checkpoint blockade therapy. *Cancer Discov*. 2018;8(9):1069–86. <https://doi.org/10.1158/2159-8290.CD-18-0367>.
3. Binnewies M, Roberts EW, Kersten K, et al. Understanding the tumor immune microenvironment (TIME) for effective therapy. *Nat Med*. 2018;24(5):541–50. <https://doi.org/10.1038/s41591-018-0014-x>.
4. Rodriguez AB, Peske JD, Woods AN, et al. Immune mechanisms orchestrate tertiary lymphoid structures in tumors via cancer-associated fibroblasts. *Cell Rep*. 2021;36(3):109422. <https://doi.org/10.1016/j.celrep.2021.109422>.
5. Engelhard VH, Rodriguez AB, Mauldin IS, Woods AN, Peske JD, Slingluff CL Jr. Immune cell infiltration and tertiary lymphoid structures as determinants of antitumor immunity. *J Immunol*. 2018;200(2):432–42. <https://doi.org/10.4049/jimmunol.1701269>.
6. Mauldin IS, Mahmutovic A, Young SJ, Slingluff CL Jr. Multiplex immunofluorescence histology for immune cell infiltrates in melanoma-associated tertiary lymphoid structures. *Methods Mol Biol*. 2021;2265:573–87. https://doi.org/10.1007/978-1-0716-1205-7_40.
7. Goldberg EP, Hadba AR, Almond BA, Marotta JS. Intratumoral cancer chemotherapy and immunotherapy: opportunities for nonsystemic preoperative drug delivery. *J Pharm Pharmacol*. 2002;54(2):159–80. <https://doi.org/10.1211/0022357021778268>.
8. Saito A, Kitayama J, Nagai R, Aizawa K. Anatomical targeting of anticancer drugs to solid tumors using specific administration routes: review. *Pharmaceutics*. 2023. <https://doi.org/10.3390/pharmaceutics15061664>.
9. Chua CYX, Ho J, Demaria S, Ferrari M, Grattoni A. Emerging technologies for local cancer treatment. *Adv Ther (Weinh)*. 2020;3(9):2000027. <https://doi.org/10.1002/adtp.202000027>.
10. Munoz NM, Williams M, Dixon K, et al. Influence of injection technique, drug formulation and tumor microenvironment on intratumoral immunotherapy delivery and efficacy. *J Immunother Cancer*. 2021. <https://doi.org/10.1136/jitc-2020-001800>.
11. Ma P, Mumper RJ. Paclitaxel nano-delivery systems: a comprehensive review. *J Nanomed Nanotechnol*. 2013;4(2):1000164. <https://doi.org/10.4172/2157-7439.1000164>.
12. Xu W, Atkinson VG, Menzies AM. Intratumoral immunotherapies in oncology. *Eur J Cancer*. 2020;127:1–11. <https://doi.org/10.1016/j.ejca.2019.12.007>.
13. Subbotin V, Fiksel G. Modeling multi-needle injection into solid tumor. *Am J Cancer Res*. 2019;9(10):2209–15.
14. Baltezor M, Farthing J, Sittenauer J, et al. Taxane particles and their use. US Patent 9,814,685. 2017.
15. Maulhardt H, Verco S, Baltezor M, Marin A, diZerega G. Local administration of large surface area microparticle docetaxel to solid carcinomas induces direct cytotoxicity and immune-mediated tumoricidal effects: preclinical and clinical studies. *Drug Deliv Transl Res*. 2022. <https://doi.org/10.1007/s13346-022-01226-2>.
16. Verco S, Maulhardt H, Baltezor M, et al. Local administration of submicron particle paclitaxel to solid carcinomas induces direct cytotoxicity and immune-mediated tumoricidal effects without local or systemic toxicity: preclinical and clinical studies. *Drug Deliv Transl Res*. 2021;11(5):1806–17. <https://doi.org/10.1007/s13346-020-00868-4>.
17. Baltezor M, Farthing J, Sittenauer J, et al. Methods for making compound particles. US Patent 9,918,957 B2. 2018.
18. Maulhardt HA, Marin AM, diZerega GS. Intratumoral submicron particle docetaxel inhibits syngeneic Renca renal cancer growth and increases CD4+, CD8+, and Treg levels in peripheral blood. *Invest New Drugs*. 2020. <https://doi.org/10.1007/s10637-020-00922-5>.
19. Maulhardt HA, Hylle L, Frost MV, et al. Local injection of submicron particle docetaxel is associated with tumor eradication, reduced systemic toxicity and an immunologic response in uro-oncologic xenografts. *Cancers*. 2019;11(4):577. <https://doi.org/10.3390/cancers11040577>.
20. Maulhardt H, Marin A, Hesselstine H, diZerega G. Submicron particle docetaxel intratumoral injection in combination with anti-mCTLA-4 into 4T1-Luc orthotopic implants reduces primary tumor and metastatic pulmonary lesions. *Med Oncol*. 2021;38(9):106. <https://doi.org/10.1007/s12032-021-01555-1>.

21. Sanchez-Correa B, Lopez-Sejas N, Duran E, et al. Modulation of NK cells with checkpoint inhibitors in the context of cancer immunotherapy. *Cancer Immunol Immunother.* 2019;68(5):861–70. <https://doi.org/10.1007/s00262-019-02336-6>.
22. Bottcher JP, Bonavita E, Chakravarty P, et al. NK cells stimulate recruitment of cDC1 into the tumor microenvironment promoting cancer immune control. *Cell.* 2018;172(5):1022–1037.e1014. <https://doi.org/10.1016/j.cell.2018.01.004>.
23. Fessenden TB, Duong E, Spranger S. A team effort: natural killer cells on the first leg of the tumor immunity relay race. *J Immunother Cancer.* 2018;6(1):67. <https://doi.org/10.1186/s40425-018-0380-4>.
24. Choucair K, Duff JR, Cassidy CS, et al. Natural killer cells: a review of biology, therapeutic potential and challenges in treatment of solid tumors. *Fut Oncol.* 2019;15(26):3053–69. <https://doi.org/10.2217/fon-2019-0116>.
25. Singh AK, Tripathi P, Cardell SL. Type II NKT cells: an elusive population with immunoregulatory properties. *Front Immunol.* 2018;9:1969. <https://doi.org/10.3389/fimmu.2018.01969>.
26. Bae EA, Seo H, Kim IK, Jeon I, Kang CY. Roles of NKT cells in cancer immunotherapy. *Arch Pharm Res.* 2019;42(7):543–8. <https://doi.org/10.1007/s12272-019-01139-8>.
27. Terabe M, Berzofsky JA. Tissue-specific roles of NKT cells in tumor immunity. *Front Immunol.* 2018;9:1838. <https://doi.org/10.3389/fimmu.2018.01838>.
28. Maulhardt HA, Marin AM, diZerega GS. Intratumoral treatment of melanoma tumors with large surface area microparticle paclitaxel and synergy with immune checkpoint inhibition. *Int J Nanomedicine.* 2024;19:689–97. <https://doi.org/10.2147/IJN.S449975>.
29. Ma X, Ding Y, Qian J, Wan M, Chen X, Xu N. Comparison of efficacy and safety of first-line chemoimmunotherapy in advanced esophageal squamous cell carcinoma: a systematic review and network meta-analysis. *J Clin Pharm Ther.* 2023;2023:3836855. <https://doi.org/10.1155/2023/3836855>.
30. Kates M, Mansour A, Lamm DL, et al. Phase 1/2 trial results of a large surface area microparticle docetaxel for the treatment of high-risk non-muscle invasive bladder cancer. *J Urol.* 2022;208(4):821–9. <https://doi.org/10.1097/JU.0000000000002778>.
31. Kates M, Mansour A, Lamm DL, et al. JU INSIGHT Phase 1/2 Trial results of a large surface area microparticle docetaxel for the treatment of high-risk non-muscle invasive bladder cancer. 2022. <https://www.aunews.net/issues/articles/2022/october-2022-online-only/ju-insight-phase-1/2-trial-results-of-a-large-surface-area-microparticle-docetaxel-for-the-treatment-of-high-risk-nonmuscle-invasive-bladder-cancer>. Accessed 15 October 2022.
32. Fu H, Zhu Y, Wang Y, et al. Identification and validation of stromal immunotype predict survival and benefit from adjuvant chemotherapy in patients with muscle invasive bladder cancer. *Clin Cancer Res.* 2018. <https://doi.org/10.1158/1078-0432.CCR-17-2687>.
33. Sharma N, Lo S, Hendifar A, et al. Response of locally advanced pancreatic cancer to intratumoral injection of large surface area microparticle paclitaxel: initial report of safety and clinical outcome. *Pancreas.* 2023. <https://doi.org/10.1097/mpa.0000000000002236>.
34. Mucciolo G, Roux C, Scagliotti A, Brugiapaglia S, Novelli F, Cappello P. The dark side of immunotherapy: pancreatic cancer. *Cancer Drug Resist.* 2020;3(3):491–520. <https://doi.org/10.20517/cdr.2020.13>.
35. Bonaventura P, Shekarian T, Alcazer V, et al. Cold tumors: a therapeutic challenge for immunotherapy. *Front Immunol.* 2019;10:168. <https://doi.org/10.3389/fimmu.2019.00168>.
36. Chen X, Zeh HJ, Kang R, Kroemer G, Tang D. Cell death in pancreatic cancer: from pathogenesis to therapy. *Nat Rev Gastroenterol Hepatol.* 2021;18(11):804–23. <https://doi.org/10.1038/s41575-021-00486-6>.
37. Guha P, Heatherton KR, O'Connell KP, Alexander IS, Katz SC. Assessing the future of solid tumor immunotherapy. *Biomedicines.* 2022. <https://doi.org/10.3390/biomedicines10030655>.
38. Cyprian FS, Akhtar S, Gatalica Z, Vranic S. Targeted immunotherapy with a checkpoint inhibitor in combination with chemotherapy: a new clinical paradigm in the treatment of triple-negative breast cancer. *Bosn J Basic Med Sci.* 2019;19(3):227–33. <https://doi.org/10.17305/bjbms.2019.4204>.
39. Demaria S, Volm MD, Shapiro RL, et al. Development of tumor-infiltrating lymphocytes in breast cancer after neoadjuvant paclitaxel chemotherapy. *Clin Cancer Res.* 2001;7(10):3025–30.
40. Champiat S, Tselikas L, Farhane S, et al. Intratumoral immunotherapy: from trial design to clinical practice. *Clin Cancer Res.* 2021;27(3):665–79. <https://doi.org/10.1158/1078-0432.CCR-20-0473>.

41. Nia HT, Munn LL, Jain RK. Physical traits of cancer. *Science*. 2020. <https://doi.org/10.1126/science.aaz0868>.
42. Nakamura Y, Mochida A, Choyke PL, Kobayashi H. Nanodrug delivery: is the enhanced permeability and retention effect sufficient for curing cancer? *Bioconjug Chem*. 2016;27(10):2225–38. <https://doi.org/10.1021/acs.bioconjugchem.6b00437>.
43. Ge R, Wang Z, Cheng L. Tumor microenvironment heterogeneity an important mediator of prostate cancer progression and therapeutic resistance. *NPJ Precis Oncol*. 2022;6(1):31. <https://doi.org/10.1038/s41698-022-00272-w>.
44. Ganesh K, Massague J. Targeting metastatic cancer. *Nat Med*. 2021;27(1):34–44. <https://doi.org/10.1038/s41591-020-01195-4>.
45. van Weverwijk A, de Visser KE. Mechanisms driving the immunoregulatory function of cancer cells. *Nat Rev Cancer*. 2023;23(4):193–215. <https://doi.org/10.1038/s41568-022-00544-4>.
46. Zhang F, Stephan SB, Ene CI, Smith TT, Holland EC, Stephan MT. Nanoparticles that reshape the tumor milieu create a therapeutic window for effective T-cell therapy in solid malignancies. *Can Res*. 2018;78(13):3718–30. <https://doi.org/10.1158/0008-5472.Can-18-0306>.
47. Mansur A, Garg T, Camacho JC, et al. Image-guided percutaneous and transarterial therapies for primary and metastatic lung cancer. *Technol Cancer Res Treat*. 2023;22:15330338231164192. <https://doi.org/10.1177/15330338231164193>.
48. Hu Y, Wei J, Shen Y, Chen S, Chen X. Barrier-breaking effects of ultrasonic cavitation for drug delivery and biomarker release. *Ultrason Sonochem*. 2023;94:106346. <https://doi.org/10.1016/j.ultsonch.2023.106346>.
49. Minchinton AI, Tannock IF. Drug penetration in solid tumours. *Nat Rev Cancer*. 2006;6(8):583–92. <https://doi.org/10.1038/nrc1893>.
50. Primeau AJ, Rendon A, Hedley D, Lilge L, Tannock IF. The distribution of the anticancer drug doxorubicin in relation to blood vessels in solid tumors. *Clin Cancer Res*. 2005;11(24 Pt 1):8782–8. <https://doi.org/10.1158/1078-0432.CCR-05-1664>.
51. Kim TK, Vandsemb EN, Herbst RS, Chen L. Adaptive immune resistance at the tumour site: mechanisms and therapeutic opportunities. *Nat Rev Drug Discov*. 2022;21(7):529–40. <https://doi.org/10.1038/s41573-022-00493-5>.
52. Zhang J, Huang D, Saw PE, Song E. Turning cold tumors hot: from molecular mechanisms to clinical applications. *Trends Immunol*. 2022;43(7):523–45. <https://doi.org/10.1016/j.it.2022.04.010>.
53. Ngwa W, Irabor OC, Schoenfeld JD, Hesser J, Demaria S, Formenti SC. Using immunotherapy to boost the abscopal effect. *Nat Rev Cancer*. 2018;18(5):313–22. <https://doi.org/10.1038/nrc.2018.6>.
54. Kim H, Venkatesulu BP, McMillan MT, et al. Local therapy for oligoprogressive disease: a systematic review of prospective trials. *Int J Radiat Oncol Biol Phys*. 2022;114(4):676–83. <https://doi.org/10.1016/j.ijrobp.2022.08.027>.
55. Weaver BA. How Taxol/paclitaxel kills cancer cells. *Mol Biol Cell*. 2014;25(18):2677–81. <https://doi.org/10.1091/mbc.E14-04-0916>.
56. Chen D, Yu J, Zhang L. Necroptosis: an alternative cell death program defending against cancer. *Biochim Biophys Acta*. 2016;1865(2):228–36. <https://doi.org/10.1016/j.bbcan.2016.03.003>.
57. Bracci L, Schiavoni G, Sistigu A, Belardelli F. Immune-based mechanisms of cytotoxic chemotherapy: implications for the design of novel and rationale-based combined treatments against cancer. *Cell Death Differ*. 2014;21(1):15–25. <https://doi.org/10.1038/cdd.2013.67>.
58. Sancho D, Joffre OP, Keller AM, et al. Identification of a dendritic cell receptor that couples sensing of necrosis to immunity. *Nature*. 2009;458(7240):899–903. <https://doi.org/10.1038/nature07750>.
59. Blankenstein T, Coulie PG, Gilboa E, Jaffee EM. The determinants of tumour immunogenicity. *Nat Rev Cancer*. 2012;12(4):307–13. <https://doi.org/10.1038/nrc3246>.
60. Kepp O, Senovilla L, Vitale I, et al. Consensus guidelines for the detection of immunogenic cell death. *Oncoimmunology*. 2014;3(9):e955691. <https://doi.org/10.4161/21624011.2014.955691>.
61. Melero I, Castanon E, Alvarez M, Champiat S, Marabelle A. Intratumoural administration and tumour tissue targeting of cancer immunotherapies. *Nat Rev Clin Oncol*. 2021;18(9):558–76. <https://doi.org/10.1038/s41571-021-00507-y>.
62. Pol J, Vacchelli E, Aranda F, et al. Trial Watch: immunogenic cell death inducers for anticancer chemotherapy. *Oncoimmunology*. 2015;4(4):e1008866. <https://doi.org/10.1080/2162402X.2015.1008866>.
63. Soliman HH. nab-Paclitaxel as a potential partner with checkpoint inhibitors in solid tumors. *Onco Targets Ther*. 2017;10:101–12. <https://doi.org/10.2147/OTT.S122974>.

64. Liu M, Tayob N, Penter L, et al. Improved T-cell immunity following neoadjuvant chemotherapy in ovarian cancer. *Clin Cancer Res*. 2022;28(15):3356–66. <https://doi.org/10.1158/1078-0432.CCR-21-2834>.
65. Javeed A, Ashraf M, Riaz A, Ghafoor A, Afzal S, Mukhtar MM. Paclitaxel and immune system. *Eur J Pharm Sci*. 2009;38(4):283–90. <https://doi.org/10.1016/j.ejps.2009.08.009>.
66. Zheng H, Zeltsman M, Zauderer MG, Eguchi T, Vaghjiani RG, Adusumilli PS. Chemotherapy-induced immunomodulation in non-small-cell lung cancer: a rationale for combination chemoimmunotherapy. *Immunotherapy*. 2017;9(11):913–27. <https://doi.org/10.2217/imt-2017-0052>.
67. Chan OT, Yang LX. The immunological effects of taxanes. *Cancer Immunol Immunother*. 2000;49(4–5):181–5. <https://doi.org/10.1007/s002620000122>.
68. Vicari AP, Luu R, Zhang N, et al. Paclitaxel reduces regulatory T cell numbers and inhibitory function and enhances the anti-tumor effects of the TLR9 agonist PF-3512676 in the mouse. *Cancer Immunol Immunother*. 2009;58(4):615–28. <https://doi.org/10.1007/s00262-008-0586-2>.
69. Chen DS, Mellman I. Oncology meets immunology: the cancer-immunity cycle. *Immunity*. 2013;39(1):1–10. <https://doi.org/10.1016/j.immuni.2013.07.012>.
70. Chen G, Emens LA. Chemoimmunotherapy: reengineering tumor immunity. *Cancer Immunol Immunother*. 2013;62(2):203–16. <https://doi.org/10.1007/s00262-012-1388-0>.
71. Saka D, Gokalp M, Piyade B, et al. Mechanisms of T-cell exhaustion in pancreatic cancer. *Cancers (Basel)*. 2020. <https://doi.org/10.3390/cancers12082274>.
72. Taniguchi Y, Shimokawa T, Takiguchi Y, et al. A randomized comparison of nivolumab versus nivolumab + docetaxel for previously treated advanced or recurrent ICI-naïve non-small cell lung cancer: TORG1630. *Clin Cancer Res*. 2022;28(20):4402–9. <https://doi.org/10.1158/1078-0432.CCR-22-1687>.
73. Cella E, Zullo L, Marconi S, et al. Immunotherapy-chemotherapy combinations for non-small cell lung cancer: current trends and future perspectives. *Expert Opin Biol Ther*. 2022;22(10):1259–73. <https://doi.org/10.1080/14712598.2022.2116273>.
74. Zamarin D, Holmgaard RB, Subudhi SK, et al. Localized oncolytic virotherapy overcomes systemic tumor resistance to immune checkpoint blockade immunotherapy. *Sci Transl Med*. 2014;6(226):226ra232. <https://doi.org/10.1126/scitranslmed.3008095>.
75. Saha D, Martuza RL, Rabkin SD. Oncolytic herpes simplex virus immunovirotherapy in combination with immune checkpoint blockade to treat glioblastoma. *Immunotherapy*. 2018;10(9):779–86. <https://doi.org/10.2217/imt-2018-0009>.
76. Bourgeois-Daigneault MC, Roy DG, Aitken AS, et al. Neoadjuvant oncolytic virotherapy before surgery sensitizes triple-negative breast cancer to immune checkpoint therapy. *Sci Transl Med*. 2018. <https://doi.org/10.1126/scitranslmed.aao1641>.
77. Samson A, Scott KJ, Taggart D, et al. Intravenous delivery of oncolytic reovirus to brain tumor patients immunologically primes for subsequent checkpoint blockade. *Sci Transl Med*. 2018. <https://doi.org/10.1126/scitranslmed.aam7577>.
78. Passaro C, Alayo Q, De Laura I, et al. Arming an oncolytic herpes simplex virus type 1 with a single-chain fragment variable antibody against PD-1 for experimental glioblastoma therapy. *Clin Cancer Res*. 2019;25(1):290–9. <https://doi.org/10.1158/1078-0432.CCR-18-2311>.
79. Zhu Y, Hu X, Feng L, et al. Enhanced therapeutic efficacy of a novel oncolytic herpes simplex virus type 2 encoding an antibody against programmed cell death 1. *Mol Ther Oncolytics*. 2019;15:201–13. <https://doi.org/10.1016/j.omto.2019.10.003>.
80. Rajani K, Parrish C, Kottke T, et al. Combination therapy with reovirus and anti-PD-1 blockade controls tumor growth through innate and adaptive immune responses. *Mol Ther*. 2016;24(1):166–74. <https://doi.org/10.1038/mt.2015.156>.
81. Schmid P, Adams S, Rugo HS, et al. Atezolizumab and nab-paclitaxel in advanced triple-negative breast cancer. *N Engl J Med*. 2018;379(22):2108–21. <https://doi.org/10.1056/NEJMoa1809615>.
82. Riano I, Abuali I, Sharma A, Durant J, Dragnev KH. Role of neoadjuvant immune checkpoint inhibitors in resectable non-small cell lung cancer. *Pharmaceuticals (Basel)*. 2023. <https://doi.org/10.3390/ph16020233>.
83. Marin-Acevedo JA, Kimbrough EO, Lou Y. Next generation of immune checkpoint inhibitors and beyond. *J Hematol Oncol*. 2021;14(1):45. <https://doi.org/10.1186/s13045-021-01056-8>.
84. Audisio A, Buttigliero C, Delcuratolo MD, et al. New perspectives in the medical treatment of non-muscle-invasive bladder cancer: immune checkpoint inhibitors and beyond. *Cells*. 2022. <https://doi.org/10.3390/cells11030357>.

85. Blanco E, Chocarro L, Fernandez-Rubio L, et al. Leading edge: intratumor delivery of monoclonal antibodies for the treatment of solid tumors. *Int J Mol Sci.* 2023. <https://doi.org/10.3390/ijms24032676>.
86. Bote H, Mesas A, Baena J, Herrera M, Paz-Ares L. Emerging immune checkpoint inhibitors for the treatment of non-small cell lung cancer. *Expert Opin Emerg Drugs.* 2022;27(3):289–300. <https://doi.org/10.1080/14728214.2022.2113377>.
87. Lee JB, Ha SJ, Kim HR. Clinical insights into novel immune checkpoint inhibitors. *Front Pharmacol.* 2021;12:681320. <https://doi.org/10.3389/fphar.2021.681320>.
88. Coosemans A, Vankerckhoven A, Baert T, et al. Combining conventional therapy with immunotherapy: a risky business? *Eur J Cancer.* 2019;113:41–4. <https://doi.org/10.1016/j.ejca.2019.02.014>.
89. Marei HE, Hasan A, Pozzoli G, Cenciarelli C. Cancer immunotherapy with immune checkpoint inhibitors (ICIs): potential, mechanisms of resistance, and strategies for reinvigorating T cell responsiveness when resistance is acquired. *Cancer Cell Int.* 2023;23(1):64. <https://doi.org/10.1186/s12935-023-02902-0>.
90. Qian X, Hu W, Yan J. Nano-chemotherapy synergize with immune checkpoint inhibitor—a better option? *Front Immunol.* 2022;13:963533. <https://doi.org/10.3389/fimmu.2022.963533>.
91. Teng MW, Galon J, Fridman WH, Smyth MJ. From mice to humans: developments in cancer immunoeediting. *J Clin Invest.* 2015;125(9):3338–46. <https://doi.org/10.1172/JCI80004>.
92. Yan Y, Kumar AB, Finnes H, et al. Combining immune checkpoint inhibitors with conventional cancer therapy. *Front Immunol.* 2018;9:1739. <https://doi.org/10.3389/fimmu.2018.01739>.
93. Wahba J, Natoli M, Whilding LM, et al. Chemotherapy-induced apoptosis, autophagy and cell cycle arrest are key drivers of synergy in chemotherapy of epithelial ovarian cancer. *Cancer Immunol Immunother.* 2018;67(11):1753–65. <https://doi.org/10.1007/s00262-018-2199-8>.
94. Pitt JM, Marabelle A, Eggermont A, Soria JC, Kroemer G, Zitvogel L. Targeting the tumor microenvironment: removing obstruction to anticancer immune responses and immunotherapy. *Ann Oncol.* 2016;27(8):1482–92. <https://doi.org/10.1093/annonc/mdw168>.
95. Workenhe ST, Nguyen A, Bakhshinyan D, et al. De novo necroptosis creates an inflammatory environment mediating tumor susceptibility to immune checkpoint inhibitors. *Commun Biol.* 2020;3(1):645. <https://doi.org/10.1038/s42003-020-01362-w>.
96. Melssen MM, Sheybani ND, Leick KM, Slingluff CL Jr. Barriers to immune cell infiltration in tumors. *J Immunother Cancer.* 2023. <https://doi.org/10.1136/jitc-2022-006401>.
97. Verco J, Johnston W, Frost M, et al. Inhaled sub-micron particle paclitaxel (NanoPac[®]) induces tumor regression and immune cell infiltration in an orthotopic athymic nude rat model of non-small cell lung cancer. *J Aerosol Med Pulm Drug Deliv.* 2019. <https://doi.org/10.1089/jamp.2018.1517>.
98. Williamson SK, Johnson GA, Maulhardt HA, et al. A phase I study of intraperitoneal nanoparticulate paclitaxel (Nanotax[®]) in patients with peritoneal malignancies. *Cancer Chemother Pharmacol.* 2015;75(5):1075–87. <https://doi.org/10.1007/s00280-015-2737-4>.
99. Mullany S, Miller D, Robison K, et al. Phase II study of intraperitoneal submicron particle paclitaxel (SPP) plus IV carboplatin and paclitaxel in patients with epithelial ovarian cancersurgery. *Gynecol Oncol Rep.* 2020;34:100627. <https://doi.org/10.1016/j.gore.2020.100627>.
100. Othman M, Patel K, Krishna S, et al. Early phase trial of intracystic injection of large surface area microparticle paclitaxel for the treatment of mucinous pancreatic cysts. *Endosc Int Open.* 2022;10(12):E1517–25. <https://doi.org/10.1055/a-1949-7730>.